Journal of Computational Electronics (2024) 23:533–539
https://doi.org/10.1007/s10825-024-02151-y

Multiband, polarization-insensitive absorber operating in the terahertz range

Ammar Armghan[1] · Lway Faisal Abdulrazak[2] · Muhammad Abuzar Baqir[3] · Muhammad Saqlain[3] · Hammad Al-Shammari[4]

Received: 31 December 2023 / Accepted: 4 March 2024 / Published online: 26 March 2024

Abstract
In this study, we analyze a thin-size metasurface-based multiband terahertz (THz) absorber with a top layer comprised of nickel-made circled plus-shaped resonators. The geometric structure of the proposed absorber consists of subwavelength size and periodically arranged nickel resonators at the top followed by substrate SiO_2 film, and the silver layer at the bottom features several high absorption bands within the 1–5-THz operating range. The proposed multiband THz absorber shows excellent absorption characteristics with perfect absorptivity, 100% at 1.5 THz, 98% at 3.2 THz, 96% at 3.72 THz, and 100% at 4.26 THz, respectively. The symmetry in the top-layer design of the unit cell shows persistence to incident waves with different polarization and makes this device independent of variation in the polarization of the waves. Besides that, surface current density analysis of the absorber illustrates that high absorption bands are achieved due to the existence of strong electric resonance in the unit cell structure. It is believed that the proposed multiband terahertz absorber with high absorption characteristics and polarization-independent behavior can be used in the field of THz shielding, THz detectors and emitters, THz sensing, and thermal imaging.

Keywords Absorber · Metasurface · Terahertz

1 Introduction

Terahertz (THz) wave covers the portion of the spectrum ranging from 0.1 to 10 THz and shows opportunities for several modern exciting applications covering bio-sensing and high-resolution imaging, chemical industries, and also supports high-speed data rate for communication systems [1–5]. THz wave features with the absorption property when it interacts with material molecules. Therefore, when THz wave interacts with the metamaterial (MM)-based structure, absorption peaks can be found over the operating band that can be used for narrowband sensing [6] and wideband absorption [7]-based applications. Several reported works show the absorption operation of the different designs-based MM devices [8–11]. For example, few studies show the operation of the wideband absorbers having ring-like structures and featuring high absorption in their operating THz range [12–15]. Besides that, for multiband operation in the THz range, several works have been reported that consist of different metasurface structures and materials and show significant high absorption based on their proposed application [7, 16–18].

From the literature, most of the MM-based THz absorbers designs are developed for single-band operation [12–15]. While focusing on achieving high absorption peaks in more than one band, several state-of-the-art works with multiband and significant high absorption features while operating in the THz range have been presented [16–18]. Therefore, these devices can be used for THz bio-sensing, high-resolution imaging, communication fields, etc.

Moving forward, several studies of multiband MM absorbers operating in the THz region have been presented [7, 16–19]. For instance, one study shows the operation of

✉ Muhammad Saqlain
saqlain@cuisahiwal.edu.pk

[1] Department of Electrical Engineering, College of Engineering, Jouf University, 72388 Sakaka, Saudi Arabia

[2] Department of Computer Science, Cihan University Sulaimaniya, Sulaimaniya, Kurdistan Region 46001, Iraq

[3] Department of Electrical and Computer Engineering, COMSATS University Islamabad, Islamabad, Pakistan

[4] Department of Mechanical Engineering, Jouf University, 72388 Sakaka, Saudi Arabia

the dual-band THz absorber with more than 80% absorption characteristics in their operating bands of 1.724 THz and 3.557 THz [19], whereas a tri-band THz absorber comprises metallic ring-shaped resonators with over 80% absorption in their operating bands of 0.337 THz, 0.496 THz, and 0.718 THz [17]. Similarly, another work presents the multiband absorber operating in the THz range up to 2 THz with significantly high absorption suitable for sensing applications [7]. Here, we present the summary of some recently published state-of-the-art studies based on the multiband absorption operation within the THz band [20–23]. For example, in [20], the authors present the operation analysis of a dual-band THz absorber made of graphene resonators that shows high absorptivity of 97.78% and 99.7% at the 2.55 THz and 5.05 THz, respectively. Similarly, authors in [21] present the study of a graphene-based square-shaped multiband THz absorber that achieved an average absorption of 99.6% at the operating frequencies of 0.49 THz, 0.65 THz, and 0.79 THz, respectively. Similarly, one study [22] shows that a tri-band THz absorber made of copper resonators features with polarization insensitivity and high absorption of 98% at 0.33 THz, 96% at 0.62 THz, and 98% at 2.08 THz, respectively, whereas authors in [23] illustrate the performance of a dual-band THz absorber made of TiNi alloy with a unit cell thickness of 29.8 µm showing the high absorption characteristics of 98.8% and 96.8% at the resonating frequencies of 0.998 THz and 1.532 THz, respectively.

For designing an absorber device, the selection of the material and design geometry are vital steps. Therefore, metals like nickel, tungsten, and gold have been widely used for THz absorber design due to their high absorption characteristics when operating in high-temperature surroundings [24–27]. Among these metals, nickel is a favorable choice for the research community to use in the making of THz absorber design due to its low cost and high absorption capability. Therefore, for keeping a view of their excellent features, nickel is considered a good selection for multiband THz absorber design. Hence, a multiband operation of the THz absorber can facilitate THz radiation-based bio-sensing and high-resolution imaging, communication fields, etc.

This study presents the investigation of a multiband metasurface-based absorber comprising of circled plus-shaped nickel resonators operating within the 1–5 THz range. The top metasurface is made of nickel-circled plus-shaped resonators with a thickness of 2 µm and placed on the silicon dioxide (SiO_2) layer of 10 µm thickness absorbing the large proportion of incident wave energy. The silver-made bottom layer does not allow the THz wave transmission. This work shows two narrowband absorption peaks with more than 85% absorption exist within 1.4–3.26 THz and one wideband absorption peak with 80% absorption in the 3.6–4.4 THz band. The symmetry of the top metasurface structure provides persistence to different polarized waves. The analysis also presents the relation of absorption characteristics versus angular variation in the incident THz waves for TE and TM modes. Moreover, the flow of current in terms of surface current density within the design structure is analyzed at several high absorption peaks to provide in-depth study of the absorption process. The high absorption peak in the narrowband region may be suitable for THz sensing, and a high absorption peak in the wideband region can be useful for THz imaging.

2 Design and theory

This section presents the design and absorption mechanism of proposed multiband absorber. The geometric dimensions of the proposed unit cell are marked in Fig. 1a. For the optimized unit cell design, period of the unit cell is represented by $P = 100$ µm, and top metasurface is made of a nickel (Ni)-made circled plus-shaped structure and

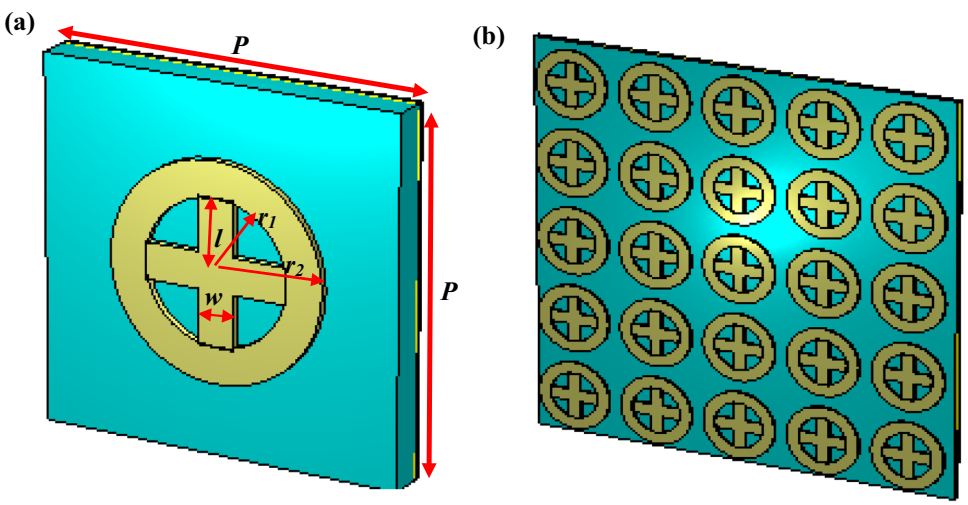

Fig. 1 Three-dimensional visualization of a unit cell with geometric details and its array **a** unit cell and its geometry detail and **b** array of the unit cell

has the following geometric dimensions: $l = 20$ μm and $w = 10$ μm, respectively, whereas the radius of inner and outer circles of this structure is represented by $r_1 = 20$ μm and $r_2 = 30$ μm, respectively. Dielectric SiO_2 layer under the top layer with a 10 μm thickness absorbs and retains maximum energy of the radiating THz waves inside its structure. The function of the bottom layer made of silver (Ag) with 1 μm thickness prevents THz wave transmission through it. Part (b) of Fig. 1 is representing the 3D view of the 5×5 array of the unit cell.

For evaluating the absorption characteristics of the proposed multiband THz absorber, the simulation work is performed in the CST software. Initially, simulation setup is made ready by applying the boundary conditions in the horizontal and vertical directions of the unit cell, and similarly, in the Z-direction, open boundary conditions are applied. As a result of simulation, we obtain S-parameters for absorption, reflection, and transmission. Using the following mathematical relation, absorption can be calculated [24].

$$A = 1 - |S_{11}|^2 - |S_{21}|^2 \tag{1}$$

From (1), absorption A is calculated in dB. The reflection coefficient represented by S_{11} and S_{21} represents the transmission coefficient.

Generally, the effect transmission coefficient is negligible due to the silver-made layer that features perfect reflection to the incident waves. Hence, we can write the simplified form of the above equation as

$$A = 1 - |S_{11}|^2 \tag{2}$$

Using (2), we can calculate the frequency-dependent absorption of the multiband THz absorber.

3 Results and discussion

In this section, first, we discuss the absorption results of different design steps involved in our proposed multiband THz absorber operating within the 1–5 THz range as shown in Fig. 2. Figure 2a shows the absorption characteristics of design-I of the unit cell that comprises a simple ring-shaped structure with inner and outer radius values of r_1 20 = μ m and r_2 30 = μ m, respectively. This design produces two absorption peaks at 1.3 THz and 3.2 THz with absorptivity of above 85%, respectively. Similarly, perfect absorption peak with 100% absorptivity is obtained at 4.6 THz. Part (b) of Fig. 2 shows the absorption characteristics of unit cell design-II (plus-shaped). This design produces multiple high absorption peaks and can be seen in their corresponding plot. These high absorption peaks within the different bands of the operating region are a result of multiple resonances within the unit cell structure. This structure design produces three high absorption narrow peaks that would be useful for sensing applications. The first absorption peak with above 80% absorptivity exists at 2.2 THz, and the second high absorption narrow peak with almost similar absorptivity is obtained at 3.2 THz operating frequency, whereas three narrowband peaks with high absorptivity of above 90% are

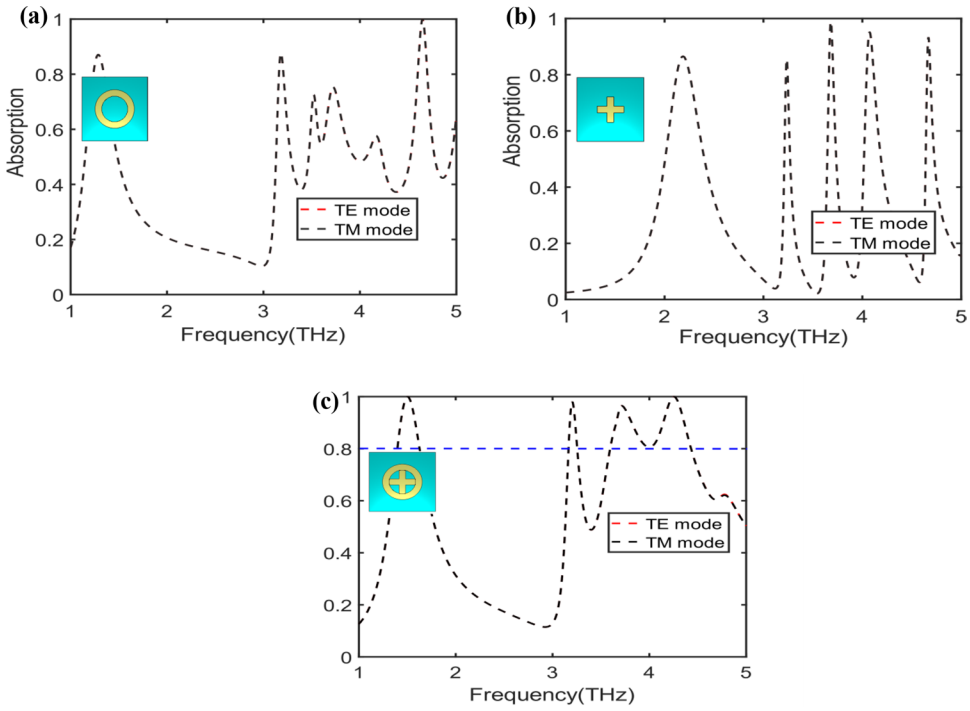

Fig. 2 Absorption characteristics results for the different unit cell designs

obtained at 3.68, 4.08, and 4.67 THz, respectively. Besides, this plus-shaped design has the four-folded symmetry and shows insensitive behavior to the polarized THz waves operated in TE and TM modes. Finally, the opted unit cell design for the proposed absorber, namely design-III, has a plus shape enclosed in a circle, and its absorption characteristics are shown in Fig. 2c. This unit cell design features a high absorption characteristic in different frequency bands. For example, the first perfect absorption peak exists at operating frequency of 1.48 THz, and the second high absorption peak of above 96% value is obtained at 3.2 THz. From the corresponding plot, the high absorption and relatively wide operating band exists within 3.5–4.5 THz region and shows absorptivity of above 80%. Moreover, TE and TM excitation modes have shown the same absorption due to the symmetry in the geometrical structures of different unit cell designs.

Here, we analyze the normalized impedance of the multiband THz absorber from the derived S-parameters. The following mathematical expression can be applied to calculate the impedance using S_{11} and S_{21} [28].

$$Z = \sqrt{\frac{\left(1+S_{11}\right)^2 - S_{21}^2}{\left(1-S_{11}\right)^2 - S_{21}^2}} \tag{3}$$

Figure 3 shows the relation of frequency-dependent impedance profile of the proposed absorber within the 1–5-THz frequency range. We can see that impedance profile (both real and imaginary parts) varies over the operating frequency window. Generally, real part of frequency-dependent impedance with unity value offers maximum absorption due to the occurrence of resonance phenomena within the absorber structure, whereas our proposed absorber impedance profile (real part) shows near-unity values at the operating frequencies of 1.48 THz, 3.2 THz, 3.7 THz, and 4.23 THz, respectively. Corresponding to the absorption curves of our proposed unit cell design (as shown in Fig. 2c) of the absorber, we can clearly see the high absorption peaks at these frequencies. Similarly, the imaginary part of the impedance shows negative values above 2.35 THz. Besides, the proposed absorber possesses symmetry property in its unit cell design, and therefore, normalized impedance remains unchanged when considering TE and TM excitation modes.

Figure 4 shows the frequency-dependent absorption of the design structure for different incidence angles. Figure 4a, b illustrates the variation in the absorption for the angular incidence of the THz wave while considering TE and TM modes, respectively. Figure 4a demonstrates the obliquity of the incident for TE mode, and it is noticed that absorptivity is much dependent on the incidence angle. Several absorption peaks are observed from the 1–5-THz frequency range due to the LSPR effect. The first absorption peak is depicted at 1.5 THz, and it is noticed that absorptivity gets reduced with the increase in incidence angle—this feature is attributed to the sensing nature of the absorber. Also, a similar absorption trend is noticed for the other absorption peaks, with the increase in θ; the absorptivity is reduced. Figure 4b

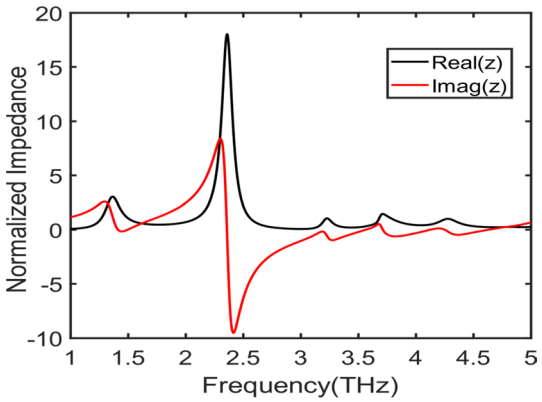

Fig. 3 Frequency-dependent impedance profile of multiband absorber operating in the THz range

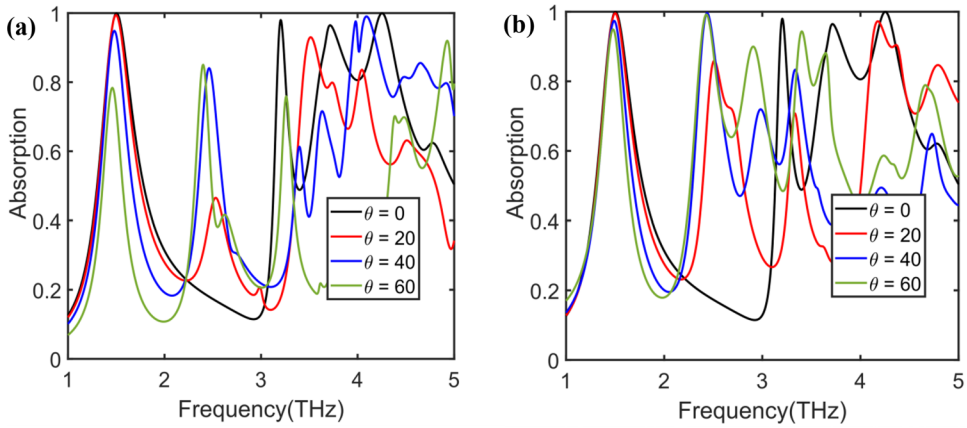

Fig. 4 Relationship of absorption characteristics of the proposed absorber with incidence angle ranging from 0 ° to 60 ° for **a** TE operation mode and **b** TM operation mode

illustrates the absorptivity features of the THz absorber for TM mode considering the obliquity of the incidence angle. For this situation, the first absorption peak is noticed at 1.5 THz; the obliquity of the incidence angle is showing a minor effect on the absorptivity of the absorber. Further multiple absorption peaks are achieved due to the multiple LSPR. The absorption peaks at higher frequencies show a profound effect on absorption by altering incidence angles. Further, the absorptivity is greatly reduced with the increase in incidence angle. The angle-dependent absorption nature of the absorber is due to the anisotropic nature of the metasurface of the THz absorber.

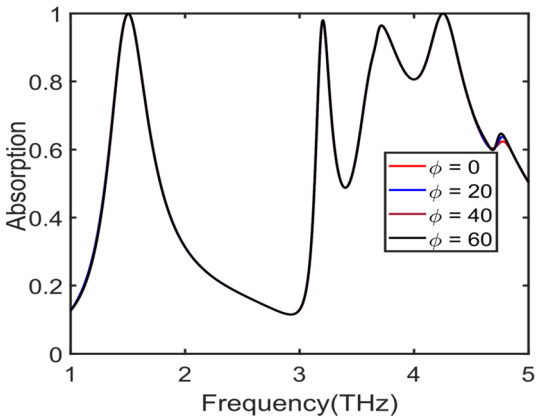

Fig. 5 Absorption relationship with polarized THz wave of different incidence angles and considering TE and TM operating modes

Next, we investigate the absorption features of the proposed absorber while varying the polarization state of incident THz waves. Figure 5 shows the absorptivity for different polarization angles considering TE and TM excitation modes. It is obvious from the corresponding plots that altering the polarization of the incident THz wave does not affect the absorption characteristics due to the four-folded symmetry of the proposed unit cell design and this feature makes this device resilient to different polarization states of the incoming THz waves. To achieve the polarization-insensitive behavior of the absorber, it is essential to design the metasurface unit cell with four-folded symmetry. This polarization-insensitive nature of the proposed device makes it useful for THz sensing and imaging. Moreover, such polarization-insensitive nature of the metasurface-based device makes it useful for beam steering and antennas.

The physical insight of the absorption through the metasurface can be understood by considering the surface current densities of the top and bottom surfaces of the structure. Figure 6 illustrates the surface current density at high absorption operating frequencies. Figure 6a, b, respectively, shows the flow of surface current within the upper layer consisting of circle-shaped resonators and a silver-made bottom layer at 1.5 THz (this high absorption frequency can be seen in Fig. 2c). The flow of current remains maximally concentrated on the surface of the circled plus-shaped resonators.

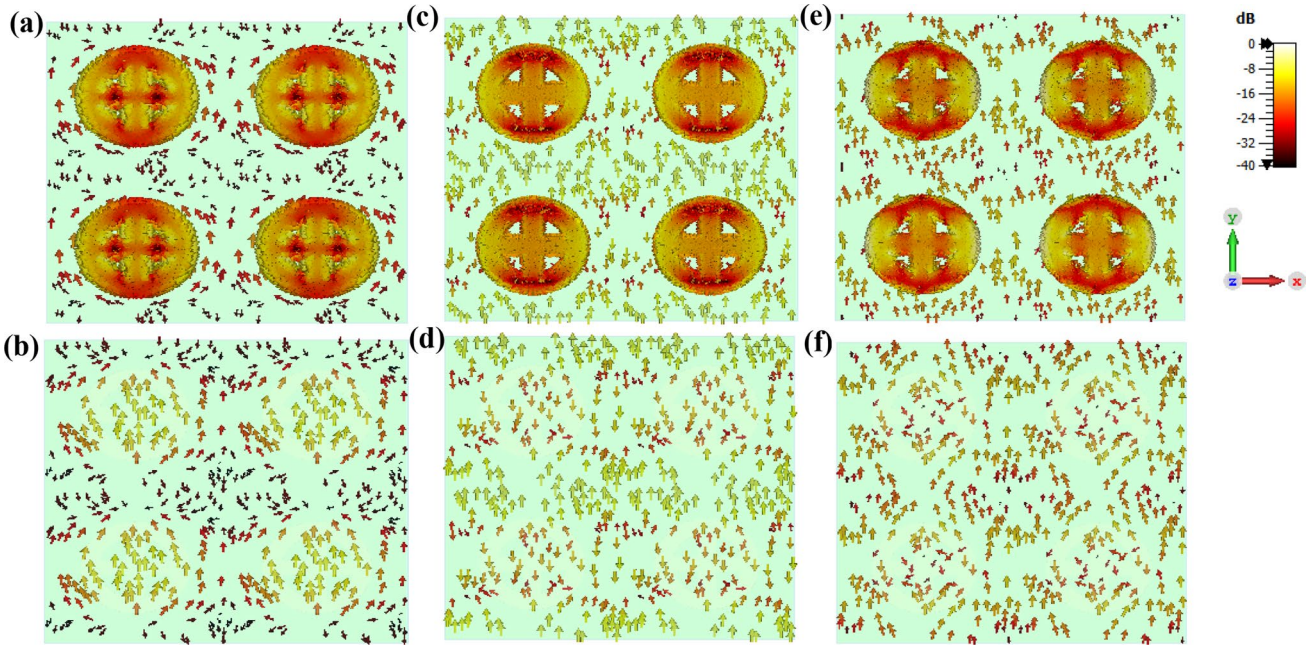

Fig. 6 Visualization of surface current density within different layers at high absorption operating frequencies **a** $f=1.5$ THz (upper layer), **b** $f=1.5$ THz (bottom layer), **c** $f=3.2$ THz (upper layer), **d** $f=3.2$ THz (bottom layer), **e** $f=4.26$ THz (upper layer), and **f** $f=4.26$ THz (bottom layer)

Table 1 Proposed multiband THz absorber performance comparison with other works

References	Unit cell thickness (μm)	High resonance frequencies (THz)	Absorption (%)	Polarization stability
Present work	13	1.5, 3.2, and 4.26	100, 98, and 100	Yes
[20]	Not given	2.55 and 5.05	97.78 and 99.7	Yes
[21]	190.5	0.49, 0.65, and 0.79	99.6 (average)	Yes
[22]	69	0.33, 0.62, and 0.82	98, 96, and 98	Yes
[23]	29.8	0.998 and 1.5328	98.8 and 96.8	Yes
[17]	10.4	0.34, 0.5, and 0.72	99.5, 86.4, and 98.4	Yes

Furthermore, it is visible that the direction of the current flow is parallel in the upper and bottom layers. Therefore, it can be concluded that the LSPR is an outcome of electric resonance. Figure 6c, d illustrates the surface current for the absorption at 3.2 THz, and it can be seen that the surface current of the top and bottom layers remains parallel which leads to the electric resonance. Further, the surface current density in the present case also remains confined on the circled plus-shaped resonator surface, and the same parallel flow of surface current within the considered layers leads to magnetic resonance. Similarly, parts (e) and (f) of Fig. 6, respectively, correspond to 4.26 THz, and similar behavior is observed.

We present a comparison of our proposed work with several recent relevant published works in Table 1. The comparison summary comprises of several important performance metrics such as unit cell thickness, high resonance operating frequencies in the THz region, absorption characteristics, and polarization stability of these devices. Among these works, our proposed work features with relatively thin-size unit cell compared to most of the listed works in Table 1. Besides, our proposed multiband THz absorber features perfect absorption at the two resonating frequencies, 1.5 THz and 4.26 THz, and hence shows better absorptivity compared to other relevant listed works. The proposed work also shows polarization stability, and its simple unit cell design helps in easy fabrication. Hence, the proposed multiband THz absorber with thin-size unit cell, high absorption characteristics, and polarization could make this device design beneficial for several applications such as THz shielding, THz detectors and emitters, and thermal imaging.

4 Conclusion

From the aforesaid discussion, a polarization-stable, thin-size metasurface-based multiband THz absorber with high absorption characteristics is analyzed. The physical mechanism of absorber has been investigated by surface current density effect at the high absorption operating frequencies, and results reveal that perfect absorption peaks with 100% absorptivity at 1.5 THz and 4.26 THz are achieved due to the existence of strong magnetic response combined with localized surface plasmon effect (LSPR). In addition, high absorption peaks in different operating THz bands are achieved due to adjustment of the geometric parameters of the unit cell. The symmetry in the unit cell design made this device polarization-independent within the 0°–90° range. The multiband high absorption characteristics and persistence to different polarization waves of the proposed device would make it useful for terahertz sensing, shielding, and imaging applications.

Acknowledgments This work was partially supported by the Higher Education Commission Pakistan (HEC) under [grant number 20-14992/NRPU/R&D/HEC/2021 2021].

Author contributions AA, LFA, and MAB conceived idea and design of the presented work. MS and HA-S put forward theory and worked out results. MAB and MS verified the analytical methods employed. AA and LFA concluded the results with support of MAB and MS. AA, LFA, MAB, and MS wrote the manuscript with support of LFA and HA-S. All authors deliberated the results and contributed to the final manuscript.

Funding No funding was obtained for this study.

Data availability Data underlying the results presented in this paper are not publicly available at this time but may be obtained from the authors upon reasonable request.

Declarations

Conflict of interest Authors have no relationships or interests that could potentially influence or bias the submitted work.

Ethical approval Not applicable for this manuscript.

References

1. Luo, C., Ling, F., Yao, G., Yao, J., Ji, J., Yue, J.: Dual-band tunable perfect metamaterial absorber in the THz range. Opt. Exp. **24**, 1518 (2016)
2. Sun, C.K., Kuo, C.C., Chuang, E.Y., Chen, H., Lu, J.T., Fu, S.C., Chen, T.H., Tseng, T.F., Lee, W.J., Huang, Y.Y.: High-sensitivity in vivo THz transmission imaging of early human breast cancer in a subcutaneous xenograft mouse model. Opt. Exp. **19**, 21552 (2011)

3. Shen, Y.C., Lo, T., Taday, P.F., Cole, B.E., Tribe, W.R., Kemp, M.C.: Detection and identification of explosives using terahertz pulsed spectroscopic imaging. Appl. Phys. Lett. **86**, 377 (2005)
4. Yoshida, H., Ogawa, Y., Kawai, Y., Hayashi, S., Hayashi, A., Otani, C., Kato, E., Miyamaru, F., Kawase, K.: Terahertz sensing method for protein detection using a thin metallic mesh. Appl. Phys. Lett. **91**, 97 (2007)
5. Wang, S., Lu, Z., Li, W., Jia, S., Zhang, L., Qiao, M., Pang, X., Idrees, N., Saqlain, M., Gao, X., Cao, X., Lin, C., Wu, Q., Zhang, X., Yu, X.: 26.8-m THz wireless transmission of probabilistic shaping 16-QAM-OFDM signals. APL Photonics **1**, 056105 (2020)
6. Sabah, C., Mulla, B., Altan, H., et al.: Cross-like terahertz metamaterial absorber for sensing applications. Pramana - J Phys **91**, 17 (2018)
7. Wang, B.X., Wang, L.L., Wang, G.Z., Huang, W.Q., Li, X.F., Zhai, X.: A broadband, polarization-insensitive and wide-angle coplanar terahertz metamaterial absorber. Eur. Phys. J. B. **87**, 98 (2014)
8. Cong, L., Tan, S., Yahiaoui, R., Yan, F., Zhang, W., Singh, R.: Experimental demonstration of ultrasensitive sensing with terahertz metamaterial absorbers: a comparison with the metasurfaces. Appl. Phys. Lett. **106**, 031107 (2015)
9. Li, F., Jiang, X., Zhao, J., Zhang, S.: Graphene oxide: a promising nanomaterial for energy and environmental applications. Nano Energy **1**(16), 488–515 (2015)
10. He, X., Gao, P., Shi, W.: A further comparison of graphene and thin metal layers for plasmonics. Nanoscale **8**, 10388–10397 (2016)
11. Lin, F., Shi, W., He, X., Zhong, X.: Investigation of graphene assisted tunable terahertz metamaterials absorber. Opt. Mater. Exp. **6**, 331 (2016)
12. Wang, B.X., Wang, G.Z.: Quad-band terahertz absorber based on a simple design of metamaterial resonator. IEEE Photon. J. **8**(6), 1–8 (2016)
13. Wang, B.X., Wang, L.L., Wang, G.Z., Huang, W.Q., Li, X.F., Zhai, X.: Metamaterial-based low-conductivity alloy perfect absorber. J. Lightwave Technol. **32**(12), 2293–2298 (2014)
14. Ma, Y., Chen, Q., Grant, J., Saha, S.C., Khalid, A., Cumming, D.R.: A terahertz polarization insensitive dual band metamaterial absorber. Opt. Lett. **36**, 945 (2011)
15. Pan, W., Yu, X., Zhang, J., Zeng, W.: d Design of broadband terahertz metamaterial absorber based on nested circle rings. IEEE Photon. Technol. Lett. **28**, 2335 (2016)
16. Le, D.T., Tong, B.T., Nguyen, T.K., Cao, T.N., Nguyen, H.Q., Tran, M.C., Truong, C.L., Bui, X.K., Vu, D.L., Nguyen, T.Q.: Polarization-insensitive dual-band terahertz metamaterial absorber based on asymmetric arrangement of two rectangular-shaped resonators. Optik **1**(245), 167669 (2021)
17. Wang, J., Lang, T., Hong, Z., Xiao, M., Yu, J.: Design and fabrication of a triple-band terahertz metamaterial absorber. Nanomaterials **11**(5), 1110 (2021)
18. Luo, Z., Ji, S., Zhao, Ji., Han, Wu., Dai, H.: A multiband metamaterial absorber for GHz and THz simultaneously. Results in Physics **30**, 104893 (2021)
19. He, X.J., Wang, Y., Wang, J., Gui, T., Wu, Q.: Dual-band terahertz metamaterial absorber with polarization insensitivity and wide incident angle. Progr. Electromagn. Res. **115**, 381–397 (2011)
20. Verma, A., Meena, O.P.: Design and investigation on polarization insensitive dual band graphene based tunable absorber for THz applications. Phys. Scripta **99**(2), 025504 (2024)
21. Han, X., Zhang, Z., Xia, Qu.: A novel miniaturized tri-band metamaterial THz absorber with angular and polarization stability. Optik **228**, 166086 (2021)
22. Hadipour, S., Rezaei, P., Norouzi-Razani, A.: Multi band square-shaped polarization-insensitive graphene-based perfect absorber. Opt. Quant. Electron. **56**(3), 1–3 (2024)
23. Zhang, K., Ma, T., Liu, J., Tian, X., Zhu, J., Tan, C.: **"**Dynamically tunable and polarization-insensitive dual-band terahertz metamaterial absorber based on TiNi shape memory alloy films. Results in Phys. **23**, 104001 (2021)
24. Rufangura, P., Sabah, C.: Dual-band perfect metamaterial absorber for solar cell applications. Vacuum **1**(120), 68–74 (2015)
25. Geldmeier, J., König, T., Mahmoud, M.A., El-Sayed, M.A., Tsukruk, V.V.: Tailoring the plasmonic modes of a grating-nanocube assembly to achieve broadband absorption in the visible spectrum. Adv. Funct. Mater. **24**(43), 6797–6805 (2014)
26. Cao, T., Wei, W.C., Simpson, R.E., Zhang, L., Cryan, M.J., Han, S., Lee, B.J.: Broadband polarization-independent perfect absorber using a phase-change metamaterial at visible frequencies. Sci. Rep. **4**, 3955 (2014)
27. Han, S., Lee, B.J.: Electromagnetic resonance modes on a two-dimensional tandem grating and its application for broadband absorption in the visible spectrum. Opt. Express **24**, A202 (2016)
28. Smith, D.R., Vier, D.C., Koschny, Th., Soukoulis, C.M.: Electromagnetic parameter retrieval from inhomogeneous metamaterials. Phys. Rev. E **71**, 036617 (2005)